CALPHAD: Computer Coupling of Phase Diagrams and Thermochemistry 44 (2014) 108–113

Contents lists available at ScienceDirect

CALPHAD: Computer Coupling of Phase Diagrams and Thermochemistry

journal homepage: www.elsevier.com/locate/calphad

Characterization of Al–Ni intermetallics around 30–60 at% Al for TLPB application

A. Urrutia [a], S. Tumminello [a,b], S.F. Aricó [c], S. Sommadossi [a,b,*]

[a] Materials Characterization, Engineering Fac., Comahue National. Univ., Buenos Aires 1400, Neuquén 8300, Argentina
[b] Materials Characterization, IDEPA (CONICET-UNCO), Buenos Aires 1400, Neuquén 8300, Argentina
[c] Materials Dep., Constituyentes Atomic Center - CNEA, Avda. del Libertador 8250, San Martín (B1650KNA), Buenos Aires, Argentina

ARTICLE INFO

Article history:
Received 15 January 2013
Received in revised form
29 July 2013
Accepted 13 August 2013
Available online 26 August 2013

Keywords:
Reactive diffusion couples
TLPB
Ni–Al
Intermetallics
Kinetics
Hardness

ABSTRACT

Interest on the Al–Ni equilibrium diagram along the latest years is associated with the attractive properties of its intermetallic phases, such as high thermal stability, high corrosion resistance and high strength to density ratio. The Transient Liquid Phase Bonding (TLPB) is a technological process which can be applied to manufacture new pieces and to perform reparations. Morphology, composition profiles, growth kinetic and hardness as a function of temperature and composition of the Intermetallic Layers (ILs) were analyzed, especially focused on solid–solid interactions during isothermal annealing in reactive diffusion couples Ni/Al (800–1170 °C). The study yields to the following association of the Al–Ni Intermetallic Phases (IPs) to the ILs: L_1 (Al_3Ni), L_2 (Al_3Ni_2), L_3 (Ni-poor AlNi), L_4 (Ni-rich AlNi) and L_5 ($AlNi_3$). The composition ranges of L_3 and L_4 are 36–46 and 53–58 at% Al, respectively. Martensitic transformation was found in the half thickness of L_4 (L_{4M} and L_{4S}) at 1170 °C. Kinetics show diffusion controlled growth for L_2 and L_5 and interface reaction control for L_4 at 800–1170 °C, while L_3 revealed a mixed kinetic behavior: parabolic at 800–1000 °C and linear at 1170 °C. The growth rate constants presented temperature dependence according to the Arrhenius model. Vickers microhardness values decrease with annealing temperature and Ni concentration for ILs, and put in evidence different mechanical properties of L_3, L_{4M} and L_{4S}.

1. Introduction

Interest on the Al–Ni equilibrium diagram [1] along the latest years is associated with the attractive properties of its Intermetallic Phases (IPs), such as high thermal stability, high corrosion resistance and high strength to density ratio. They have a wide range of engineering applications, from high temperature environmental corrosion resistant coatings to structural material for turbine blades [2]. Processes involving Ni-base superalloys require thorough thermodynamic and kinetic descriptions to make possible its prediction and design. Even though Al–Ni is often mentioned as a "well characterized" system, we still face challenges related to comprehension of basic atomic mechanisms which control phase transformations involved in technological applications, mostly far from the equilibrium [2].

The remarkable amount of basic information, available on Al–Ni, turns it into a prototype system in several areas of investigation. Synergy between experimental data and computational modeling will certainly contribute to a better understanding of this system. *Ab initio* as well as CALPHAD are essential modeling techniques to understand kinetics and thermodynamic behavior. The thermodynamic assessment of the Al–Ni system was performed [3]. Recently, thermodynamic parameters were converted to the four sublattice model [4], becoming more complex models with the evolution of technology.

Reactive diffusion couple experiments are usually used to study IPs growth. The phase growing sequence depends on the temperature, reaction time, composition gradients, interfacial surface energies, Gibbs free energies, and other phases [5]. Equilibrium IPs have been reported, as well as the presence of IPs not predicted in the equilibrium diagram [5–11]. Furthermore, special attention is drawn to the central portion of the Al–Ni equilibrium diagram, i.e. from 36 to 56 at%Al where AlNi phase exists with B2 (CsCl type) structure. One of the main features of this IP is the complex defect structure which extends from stoichiometric composition. Hence alloys on this side of the stoichiometric composition contain an unusually large number of lattice vacancies. It was found a strong influence of composition on formation enthalpies, thermal conductivity, molar volume, lattice parameters, densities and diffusion coefficient, leading to split phases in two regions of different

* Corresponding author at: Materials Characterization, Engineering Fac., Comahue National. Univ., Buenos Aires 1400, Neuquén 8300, Argentina. Tel.: +54 2994490300.
E-mail addresses: silvana.sommadossi@fain.uncoma.edu.ar, ssommadossi@gmail.com (S. Sommadossi).

0364-5916/$ - see front matter © 2013 Elsevier Ltd. All rights reserved.
http://dx.doi.org/10.1016/j.calphad.2013.08.004

compositions [12–16]. Another important characteristic observed nearby the central portion of the Al–Ni system, enhancing the technological interest, is the martensitic transformation in diffusion couples experiences after quenching and the martensitic structure $L1_0$ [9,17–19] with thermoelastic properties.

Most of the diffusion couples experiments reported for this system consist in annealing Ni in contact with Ni–Al intermetallics or two Al–Ni intermetallics by solid/solid interaction, then one or two phases start to grow in between. Unfortunately, these cases are sometimes far away from the technological process, where various processes run simultaneously, influencing each other. The Transient Liquid Phase Bonding (TLPB) is a technological process which can be applied to manufacture new pieces and to perform reparations [20]. The TLPB applied to this system, can be understood partially as a reactive diffusion couple Ni/Al, where IPs are formed isothermally in the interconnection zone (IZ) by liquid/solid and solid/solid interactions, which may occur simultaneously or sequentially [8,21]. Therefore, the properties of this intermetallic layers (ILs) formed in the IZ are responsible for the bond reliability.

The aim of this work is to characterize in detail morphology, composition profiles, growth kinetic parameters, and hardness of ILs as a function of process temperature and composition for the phases developed in the technological process TLPB for a wide temperature range (800, 900, 1000 and 1170 °C). The complete phase growing sequence, starting from Al richest phases to Ni richest ones, and the influence of simultaneous/competitive growing will be analyzed. The study will be focused especially in the composition range of 40–60 at% Al, in order to evaluate the technological implications (microstructure, kinetic, hardness, etc.) of the NiAl splitting effect.

2. Methodology

Reactive diffusion couples were assembled with Ni substrates and Al as filler material, both polycrystalline materials of high purity (4 N). Rectangular sections of Ni sheets of 1 mm thickness and mirror like surface finishing were obtained by using a high precision diamond saw (Struers) and diamond paste down to 15 μm. Al foils ranging from 200 to 500 μm thick were located between Ni sheets using a fastening system. Quartz slips were used as inert markers between Al and Ni, to indicate the original interface and to ensure constant thickness in the IZ. The assembly was placed in a quartz tube under an Ar controlled atmosphere to avoid oxidation reactions. Several isothermal annealing were carried out at selected temperatures: 800, 900, 1000 and 1170 °C, varying the annealing time in the subsequent stages. Cold water was used to stop each annealing stage to obtain a high cooling rate. Cross-sections of the reactive diffusion couples were prepared by using 0.25 μm diamond paste as the last polishing step. Chemical etching solution 20% HCl, 20% H_2O and 60% HNO_3 was used to reveal the microstructure of the IZ.

Morphologic analyses as well as kinetic measurements were performed using an optical microscope (Nikon 80i) with polarized light linked to digital image analyzer software (NIS Elements). Thickness of the ILs was determined as average value of at least five measurements for each layer and annealing time. Microhardness determinations for each IL in the IZ were performed using a Vickers microhardness tester (Wolpert) from an average of at least five indentations. Different loads were used to avoid distortion effects produced by deformations close to interfaces or other indentations. Concentration profiles of the ILs were analyzed using electron microscopy techniques SEM-EDS (Philips) and SEM-WDS (Cameca).

3. Results and discussion

3.1. Intermetallic layers identification

A layered morphology for the IZ was obtained after reactive diffusion couple experiment (or TLPB process) at all annealing temperatures (800, 900, 1000, 1170 °C) and times. A typical multilayer sequence is shown in Fig. 1 on a chemical etched IZ cross section obtained after 1:45 h under 800 °C. According to the appearance sequence, the ILs were named from L_1 to L_5. The first IL formed is L_1, which cannot be seen in the micrograph (due to scale reasons). Both L_1 and L_2 were previously characterized [21]. L_1 reveals faceted morphology (liquid–solid interaction) whereas L_2 grows as homogeneous layer with smooth interfaces (solid–solid interaction). Previous WDS chemical analyses on L_1 and L_2 revealed that these ILs, in agreement with the phase diagram [1], correspond to the equilibrium IPs: Al_3Ni and Al_3Ni_2, respectively. The next layers, L_3 to L_5, developed with smooth interfaces (solid–solid interaction), which are stable over a wide range of temperatures (800–1170 °C). At temperature range 900–1000 °C the first IL which forms between the Ni and Al is L_2, with a lobular morphology at L_2/Al (liquid–solid interaction) and a smooth morphology at interface L_3/L_2 (solid–solid interaction). Finally, L_3 developed in contact with molten Al at 1170 °C as the first IL.

At 800 °C the Al–Ni equilibrium phase diagram predicts the existence of Al_3Ni, Al_3Ni_2, AlNi and $AlNi_3$, i.e. 4 equilibrium IPs. However 5 ILs can be clearly distinguished in the IZ cross section of Fig. 1 at the same temperature. This experimental fact may indicate a contradiction with the equilibrium phase diagram, suggesting the presence of an additional IL. However, this fact could be probably explained due to the well known AlNi phase splitting because of its excess of defect structural phenomena [13]. The thickness of L_3 corresponds to a single grain which grows as a column with grain boundaries perpendicular to the original bond interface, as can be seen in Fig. 2 for a chemical etched IZ cross section obtained after 10 min under 1170 °C. Some amount of L_2 can also be seen in Fig. 2, even Al_3Ni_2 should not form at 1170 °C according to the phase diagram. However it precipitates during cooling because the molten Al was supersaturated in Ni at 1170 °C. The different grain orientations in both L_3 and L_4 are exposed. The grain boundaries of L_3 continue their trajectory along L_3/L_4 interface setting the grain limits on the growing L_4. Smooth solid–solid interfaces L_3/L_4 and L_4/L_5 are also evident in the optical micrograph. Here is also evident a distinctive yellow intensity inside L_4 parallel to the original interfaces. By longer annealing

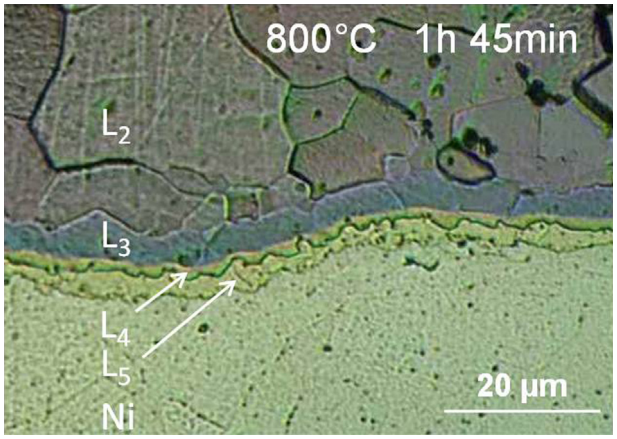

Fig. 1. Optical micrograph of an IZ obtained after 1:45 h under 800 °C showing four ILs (L_2–L_5).

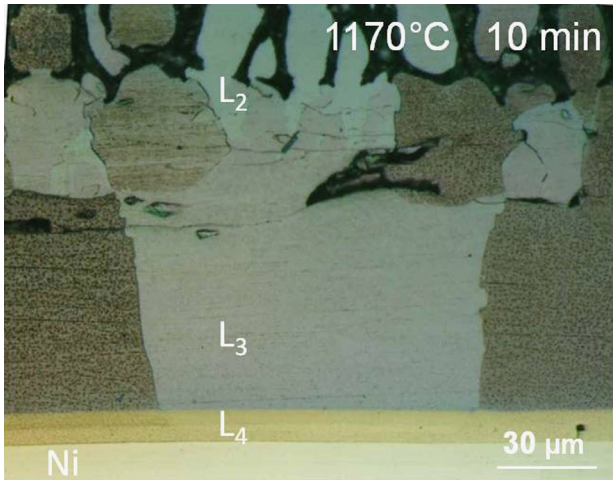

Fig. 2. Optical micrograph of a chemical etched IZ annealed at 1170 °C during 10 min indicating grain orientations and interfaces for both L_3 and L_4.

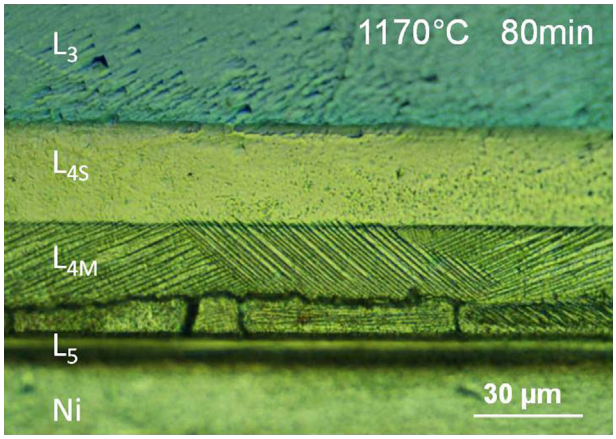

Fig. 3. Optical micrograph of an IZ obtained after 80 min of annealing at 1170 °C, L_4 shows two types of morphologies, smooth L_{4S} and martensitic L_{4M}.

times (80 min, 1170 °C), became more evident when two different morphologies, i.e. smooth (L_{4S}) and striped (L_{4M}) appear in the IZ (Fig. 3). The L_{4M} microstructure may correspond to the typical martensitic morphology, which was reported previously for this system [9,17–19]. It is worth noting that the martensitic microstructure strictly appears close to the L_5 and only covers half of the total thickness of L_4, which is very attractive for technological applications due to the typical martensitic thermoelastic nature. Further structural characterization as a function of annealing temperature and cooling rate is required to be conclusive about this transformation (L_{4S}–L_{4M}).

Chemical composition profiles were performed on several samples to characterize each IL at different annealing temperatures. The chemical profile and the SEM-BSE micrograph indicating the scanning zone for an IZ after 20 min of annealing at 1170 °C is presented in Fig. 4. Starting the line scan from Ni side, it can be seen that the average composition for L_5, L_{4M}, L_{4S} and L_3 was 30, 37, 42 and 54 at%Al, respectively. It is important to notice that L_{4S} shows a composition gradient instead of a constant composition step tendency like the other ILs. All experimental values are overlapped on the Al–Ni phase diagram in Fig. 5. Dashed lines denote the annealing temperatures used in this work, black circles represent the WDS results and rhombs the EDS results. It is noteworthy that L_3 is associated to the Ni-poor AlNi phase, whereas L_4 is related to the Ni-rich AlNi phase [9,13]. However, there is evidence of the existence of the phase Al_4Ni_3 (spatial group Ia3d) within the Ni-poor NiAl

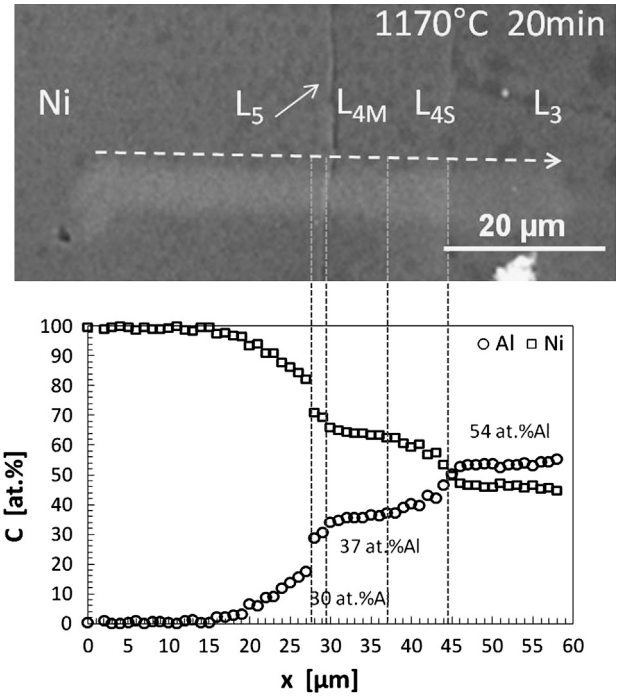

Fig. 4. Chemical composition profile by SEM-WDS for an IZ obtained after 10 min under 1170 °C.

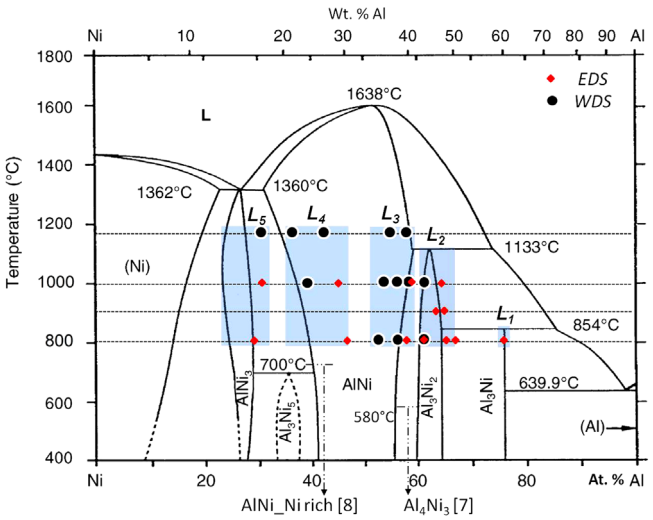

Fig. 5. Equilibrium phase diagram Al–Ni [1] indicating the experimental chemical composition values for each IL at different annealing temperatures.

region, which was identified at 530 °C by powder diffraction [7]. The crystallographic structure corresponds to Ga_4Ni_3 prototype [22], which can be converted to B_2 type (AlNi structure) by adding Ni atoms in the sites (16b) of the spatial group Ia3d. Further structural determinations on L_3 will confirm these associations.

3.2. Intermetallic layers growth kinetics

In order to model the growth of a homogeneous IL, the following general exponential law can be used [23]:

$$\Delta x = kt^n \tag{1}$$

Its equivalent logarithmic form is more adequate for experimental data fitting, since by using linear regression it is possible to obtain

n and k parameters:

$$\log(\Delta x) = n\log(t) + \log(k) \quad (2)$$

where Δx= layer thickness; t= annealing time; k= growth rate constant; n= exponential factor.

The exponential factor n is associated with the controlling mechanism of the IL growing process. Values tending to 0.5 are indicative of diffusion control, whereas values tending to 1 reveal interface reaction control.

The measured thicknesses of each IL after each annealing stage were fitted using Eq. (2) for all temperatures. In this way n parameters were obtained and after their evaluation, i.e. compared with 0.5 or 1, the experimental data were forced to fit Eq. (1) using n=0.5 or 1 in order to obtain a growth rate constant k for diffusion or reaction control, respectively. It is important to notice that the IL can present different behaviors, i.e. sequential growth, simultaneous growth and IL decreasing through decomposition. The last fact was observed for the whole temperature range, where the Ni-poorest IL starts to be consumed at expense of the other ILs when the Al source of the reactive diffusion couples disappears. It can be seen in Fig. 6 for a reactive diffusion couple, how L_3 grows till a certain annealing time and then starts to decrease at expense of the Ni-richest ILs. The growth of L_{4S} and L_{4M} can be also distinguished from the global L_4 growth. Qualitatively, the growth rates for L_{4S} and L_{4M} are very similar but lower than the one for L_3. The growth rate constants for the ILs at all temperatures and their fitted Arrhenius parameters are gathered in Table 1. There are different mechanisms controlling the IL growth. A parabolic behavior was observed for L_2 and L_5 from 800 to 1170 °C, whereas L_4 shows a linear thickness increase with annealing time from 800 to 1170 °C. A particular behavior was observed for L_3 since it changes from linear growth to parabolic ones at 1170 °C, i.e. when L_3 changes its growth from solid–solid interaction to liquid–solid ones. The kinetics show how L_3 (NiAl Ni-poor) and L_4 (NiAl Ni-rich) behave as they were different IPs. The temperature influence on the growth rate constant follows the Arrhenius phenomenological model as the good fitting in Fig. 7 shows. The k value for L_3 at 1170 °C was not considered for the fitting because of the already mentioned growth mechanism change.

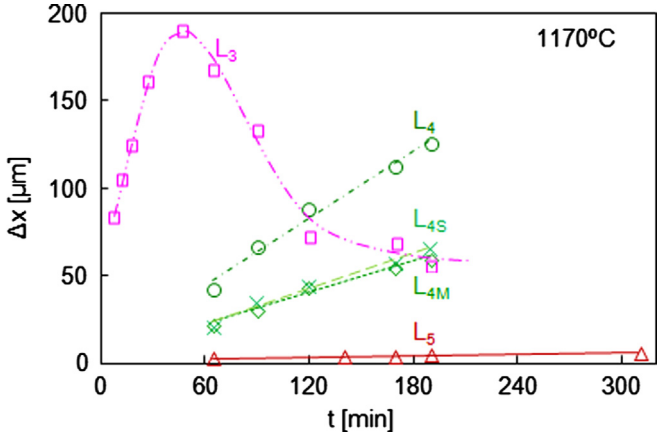

Fig. 6. Layer thickness vs. annealing time at 1170 °C for all ILs present in the IZ.

3.3. Microhardness

The average Vickers microhardness values are summarized in Table 2 as a function of annealing temperature and ILs. On one side, the temperature increase has a softening effect on the hardness values for each IL. On the other side, the Ni content increase also produces softening at all annealing temperatures. It was found that the annealing time has a negligible influence on the hardness values. These findings are depicted in Fig. 8 for all the ILs present in an IZ annealed at 1170 °C. These values put in evidence the different mechanical properties of L_3, L_{4M} and L_{4S}. The presence of two microstructures L_4 is reflected as different indentation areas shown in Fig. 9, where L_{4M} is around 14% softer

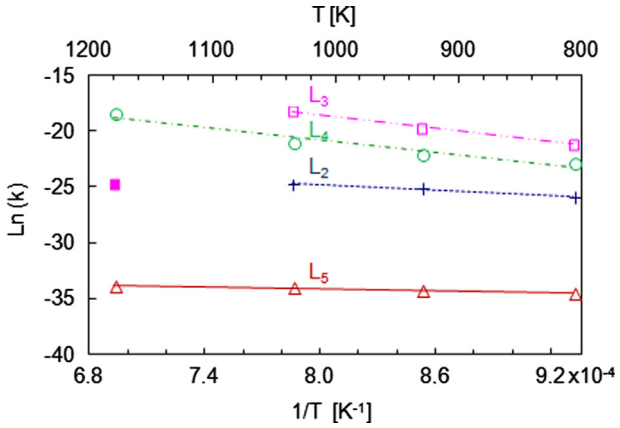

Fig. 7. Temperature dependence of the growth rate constants fitted by the Arrhenius model for all ILs. Filled square for L_3 indicates growth mechanism change from linear dependence to parabolic one.

Table 2
Average Vickers microhardness values for the ILs at 800, 900, 1000 and 1170 °C.

	Hardness values, HV 0.05			
Layers	800 °C	900 °C	1000 °C	1170 °C
L_2	952 ± 20	908 ± 67	889 ± 22	–
L_3	799 ± 22	762 ± 56	679 ± 63	584 ± 62
L_4	628 ± 20	615 ± 07	438 ± 29	422 ± 31
L_{4S}	–	–	–	435 ± 15
L_{4M}	–	–	–	385 ± 18
L_5	490 ± 11	488 ± 32	400 ± 29	334 ± 08

Table 1
Average growth rate constants for the ILs at 800, 900, 1000 and 1170 °C and Arrhenius parameters.

Growth rate constants, k					*Arrhenius parameters*	
Layers	800 °C	900 °C	1000 °C	1170 °C	E_a [kJ/mol]	k_0
L_2	5.8×10^{-12} m²/s	1.2×10^{-11} m²/s	1.8×10^{-11} m²/s		64.7	8.5×10^{-09} m²/s
L_3	6.6×10^{-10} m/s	2.8×10^{-09} m/s	1.3×10^{-08} m/s	1.7×10^{-11} m²/s[a]	167.3	8.7×10^{-02} m/s
L_4	1.3×10^{-10} m/s	2.5×10^{-10} m/s	8.1×10^{-10} m/s	1.0×10^{-08} m/s	154.7	2.8×10^{-03} m/s
L_5	1.0×10^{-15} m²/s	1.4×10^{-15} m²/s	1.6×10^{-15} m²/s	1.9×10^{-15} m²/s	20.9	1.1×10^{-14} m²/s

[a] L_3 shows diffusion controlled growth mechanism at 1170 °C.

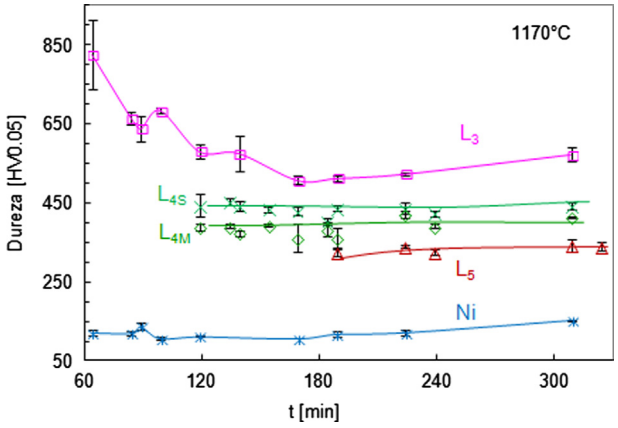

Fig. 8. Vickers microhardness profiles vs. annealing time for ILs and Ni substrate at 1170 °C.

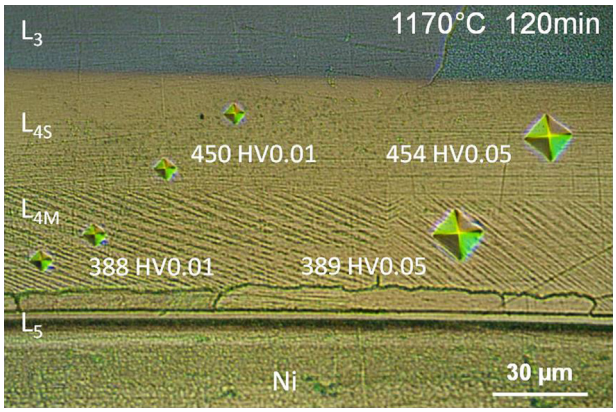

Fig. 9. Microhardness Vickers indentations using different loads on an etched IZ obtained after 120 min under 1170 °C, indicating hardness difference for L_{4S} and L_{4M}.

than the L_{4S}. There is a lack in literature of detailed hardness information for all the IPs of the Al–Ni system in order to make comparison. However, the results for L_2 are in good agreement with other work [24].

It is noteworthy that the general mechanical behavior of the multilayer IZ was quite stable considering the large number of rapid heating–cooling cycles suffered during the kinetic study, since no interface defects, cracks or fractures were found in the IZ. This fact indicates that the residual stresses, which normally appear at interfaces in multilayer growing systems, are not strong enough to produce failure, e.g. layer delamination, which is quite valuable for any technological application.

4. Conclusions

A detailed description of the phase transformations occurring in a reactive diffusion couple Ni/Al experiment along a wide temperature range (800–1170 °C) was presented. The experimental findings obtained in this work show evidence of the formation of maximal five ILs in Al/Ni reactive diffusion couples depending on the annealing temperature (800–1170 °C). The IL identification study yields to associate equilibrium Al–Ni IPs with the ILs as follow: L_1 (Al_3Ni), L_2 (Al_3Ni_2), L_3 (Ni-poor AlNi), L_4 (Ni-rich AlNi) and L_5 ($AlNi_3$). The composition ranges of L_3 and L_4 are 36–46 and 53–58 at%Al, respectively. Two substantially different morphologies were observed for L_4 at 1170 °C, namely L_{4S} and L_{4M}, the latter suggests martensitic transformation. Kinetics show diffusion controlled growth for L_2 and L_5 and interface reaction for L_4 in the annealing temperature range 800–1170 °C, while L_3 revealed a mixed kinetic behavior: parabolic at 800–1000 °C and linear at 1170 °C. The growth rate constants presented temperature dependence according to the Arrhenius model. Vickers microhardness values decrease with annealing temperature and with Ni concentration for ILs. All microstructure, kinetic and microhardness results show a quite distinctive behavior for L_3 and L_4, which are important for theoretical and technological issues. Structural investigation by means of diffraction techniques (synchrotron or neutron) and especially local characterization, such as TEM or EBSD, are required in order to be conclusive on phase stability for L_3, L_4 and L_{4M}.

Acknowledgments

The authors are grateful to the Science and Technological National Agency for the financial support through project PICT 2010-2176 RAICES - FONCyT.

Appendix A. Supplementary materials

Supplementary materials associated with this article can be found in the online version at http://dx.doi.org/10.1016/j.calphad.2013.08.004.

References

[1] H. Okamoto, Al–Ni (Aluminum–Nickel), J. Phase Equilibria 14 (1993) 257–259.
[2] D.B. Miracle, The physical and mechanical properties of Ni–Al, Acta Metall. Mater. 41 (3) (1993) 649–684.
[3] I. Ansara, N. Dupin, H.L. Lukas, B. Sundman, Thermodynamic assesment of the Al–Ni system, J. Alloys Compd. 247 (1997) 20.
[4] X.G. Lu, B. Sundman, J. Ågren, Thermodynamic assessments of the Ni–Pt and Al–Ni–Pt systems, Calphad 33 (2009) 450–456.
[5] A.S. Edelstein, R.K. Everett, G.Y. Richardson, S.B. Qadri, E.I. Altman, J.C. Foley, et al., Intermetallic phase formation douring annealing of Al/Ni multilayers, J. Appl. Phys. 76 (1994) 7850–7859.
[6] R.J. Tarento, G. Blaise, Studies of the first steps of thin film interdiffusion in the Al–Ni system, Acta Metall. 37 (1989) 2305–2312.
[7] M. Ellner, S. Kek, B. Predel, Ni3Al4—a phase with ordered vacancies isotypic to Ni_3Ga_4, J. Less-Common Met. 154 (1989) 207–215.
[8] G.A. López, S. Sommadossi, P. Zieba, W. Gust, E.J. Mittemeijer, Kinetic behaviour of diffusion-soldered Ni/Al/Ni interconnections, Mater. Chem. Phys. 78 (2002) 459–463.
[9] U. Shoo, M. Hirscher, H. Mehrer, Growth of intermetallic phases and interdiffusion in the Al–Ni system, Defect Diffusion Forum 143–147 (1997) 631–636.
[10] K. Barmak, C. Michaelsen, G. Lucadmno, Reactive phase formation in sputter-deposited Ni/Al multilayer thin films, J. Mater. Res. 12 (1997) 133–146.
[11] A.S. Edelstein, R.K. Everett, G.Y. Richardson, S.B. Qadri, J.C. Foley, J. H. Perepezko, Reaction kinetics and biasing in Al/Ni multilayers, Mater. Sci. Eng. A 195 (1995) 13–19.
[12] A. Paul, A.A. Kodentsov, F.J.J. Van Loo, On diffusion in the beta-NiAl phase, J. Alloys Compd. 403 (2005) 147–153.
[13] F.M. d'Heurle, R. Ghez, Reactive diffusion in a prototype system: nickel–aluminum I: Non-constant diffusion coefficient, Thin Solid Films 215 (1992) 19–25.
[14] K. Rzyman, Z. Moser, Calorimetric studies of the enthalpies of formation of Al_3Ni_2, AlNi and $AlNi_3$, Prog. Mater. Sci. 49 (2004) 581–606.
[15] P. Nash, O. Kleppa, Composition dependence of the enthalpies of formation of NiAl, J. Alloys Compd. 321 (2001) 228–231.
[16] J.C. Zhao, X. Zheng, D.G. Cahill, Thermal conductivity mapping of the Ni–Al system and the beta-NiAl phase in the Ni–Al–Cr system, Scr. Mater. 66 (2012) 935–938.
[17] Y.K. Au, C.M. Wayman, Thermoelastic behavior of the martensitic transformation in beta NiAl alloys, Scr. Metall. 6 (1972) 1209–1214.
[18] S. Chakravorty, C.M. Wayman, The thermoelastic martensitic transformation in beta' Ni–Al alloys: I. crystallography and morphology, Metall. Trans. A 7 (1976) 555–568.
[19] S. Chakravorty, C.M. Wayman, The thermoelastic martensitic transformation in beta' Ni–Al alloys: II. Electron microscopy, Metall. Trans. A 7 (1976) 569–582.
[20] W.D. Mac Donald, T.W. Eagar, Transient liquid phase bonding, Annu. Rev. Mater. Sci. 22 (1992) 23–46.

[21] S. Tumminello, S. Sommadossi, Growth kinetics of intermetallic phases in transient liquid phase bonding process (TLPB) in Al /Ni system, Defect Diffusion Forum 323–325 (2012) 465–470.
[22] Naval Research Laboratory. ⟨http://cst-www.nrl.navy.mil/lattice/alloys/index.html⟩. 2004.
[23] G.V. Kidson, Some aspects of the growth of diffusion layers in binary systems, J. Nucl. Mater. 3 (1961) 21–29.
[24] H.Y. Kim, D.S. Chung, S. Hong, Reaction synthesis and microstructures of NiAl/Ni micro-laminated composites, Mater. Sci. Eng. A 396 (2005) 376–384.